Measuring the Emergence of Urban Cohesion in Early Settlements: A Spatial Agent-Based Model*

Luca Pasquino[1,†], Niccolò Kaddera[1,†], Leonardo Mascagni[1,2], Andrea Monoli[1,2] and Francesco Bertolotti[1,3,*,†]

[1]Intelligence, Complexity, and Technology Lab (ICT Lab), University Cattaneo – LIUC, Italy
[2]School of Industrial Engineering, Cattaneo University – LIUC, Italy
[3]Università Cattolica di Milano, Department of Philosophy, L. Gemelli 1 - 20123 Milano, Italy

Abstract

The transition from dispersed agricultural settlements to cohesive urban agglomerations represents a fundamental phase in the evolution of any human socio-spatial organization. This paper investigates such a transition through a spatially explicit Agent-Based Model designed to simulate early agricultural societies, one of the simple case study of these phenomena. In the model, autonomous households manage agricultural fields, satisfy metabolic needs, expand their productive infrastructure, and undergo demographic scission when internal population thresholds are exceeded. We introduce an Urban Cohesion Index, a normalized measure that combines Euclidean distances among households with their topological proximity rankings to capture the relational structure of settlements and allows the identification of phase transitions from dispersed rural patterns to cohesive urban cores. Results show that urbanization does not emerge as a gradual consequence of demographic growth, but rather as a non-linear transition triggered by spatial saturation, ecological constraints, and cooperation requirements. Moreover, results indicate that small household capacity, constrained settlement radius, and broader cooperation distance strongly favor spatial clustering, while oversized households and unconstrained demographic growth tend to produce fragmentation, resource depletion, and systemic collapse.

Keywords

LaTeX class, paper template, paper formatting, CEUR-WS

1. Introduction

The transition from dispersed agricultural settlements to dense urban agglomerations represents a crucial turning point in the evolution of human spatial and social organization [1]. This profound reorganization is not merely the result of linear demographic growth, but emerges from the interaction between environmental constraints, resources management, and the dynamics of social cooperation [2]. Historically, the need to optimize agricultural labor and manage the ecological lifecycle of arable land has confronted individual family units with a fundamental dilemma: to maintain absolute spatial and productive autonomy, facing the risks of soil depletion alone, or to converge toward cooperative strategies [3, 4]. Spatial convergence fosters the sharing of caloric surplus and risk mitigation, effectively triggering the first rudimentary processes of urbanization [5, 6].

To fully understand the mechanics of this non-linear transition, it could be useful to move beyond traditional aggregated approaches in favor of a bottom-up perspective [7]. Agent-Based Models (ABMs) have proven to be an exceptionally effective analytical tool in the study of complex adaptive systems [8, 9, 10]. They allow researchers to observe how structured macroscopic patterns, such

Woodstock'22: Symposium on the irreproducible science, June 07–11, 2022, Woodstock, NY

*You can use this document as the template for preparing your publication. We recommend using the latest version of the ceurart style.

*Corresponding author.
†These authors contributed equally.
kulyabov-ds@rudn.ru (L. Pasquino); i.tiddi@vu.nl (N. Kaddera); le21.mascagni@stud.liuc.it (L. Mascagni); an26.monoli@stud.liuc.it (A. Monoli); fbertolotti@liuc.it (F. Bertolotti)
https://kmitd.github.io/ilaria/ (N. Kaddera)
0000-0001-7116-9338 (N. Kaddera); 0000-0003-1274-9628 (F. Bertolotti)

as urban density, spontaneously emerge from decentralized, micro-founded decisions [11]. As extensively demonstrated in the literature for modeling social dilemmas [12], collective choices [13], and epidemiological dynamics [14], the computational approach of ABMs captures local interactions that analytical models struggle to describe [15]. Applied to spatial economics and computational archaeology, this method enables the explicit mapping of the topological evolution of settlements [16, 17].

To address these complex dynamics, this paper introduces a spatially explicit ABM [18] specifically designed to simulate the socio-ecological evolution of early agricultural societies [16]. In our simulated environment, autonomous family units act as the primary actors. They are tasked with managing the life cycle of agricultural fields, continuously evaluating their collective caloric needs, and expanding their agricultural infrastructure. In the model, spatial dispersion is a deterministic consequence of demographic pressure: when a family reaches its maximum structural capacity due to population growth, it is forced to undergo fission, expelling members to establish a new, independent settlement. A central challenge in studying these simulated spatial dynamics is to fid a generative process [19] that results in a urban-like settlement, and measuring according. Traditional metrics, such as simple aggregate population density, often fail to capture the true topological structure and the degree of clustering within a settlement [20, 21].

To overcome this analytical limitation and accurately evaluate the transition from dispersed farming to agglomerated living, we propose the Urban Cohesion Index. This metric goes beyond absolute physical distances by cross-referencing Euclidean spatial measurements with topological density—specifically, the ordinal rank of distances between households, and provides a normalized, highly sensitive measure of spatial clustering. This allows to quantitatively specify the conditions—such as variations in labor productivity or maximum cooperation distance—that trigger the structural collapse of isolated, demographically-driven households into cohesive, centralized urban cores.

The structure of this paper is organized as follows. Section 2 details the model's methodological architecture, describing the core entities, the metabolic and ecological mechanics, the demographic fission constraints, and the mathematical formalization of the Urban Cohesion Index. Section 3 outlines the experimental setup, detailing the parameter space and the batch simulation protocols utilized for data generation. Section 4 presents the results of the macroscopic data analysis, highlighting the phase transitions in spatial agglomeration and the systemic triggers of urbanization. Finally, Section 5 discusses the implications of these findings for broader theories of urban development and suggests potential avenues for future research.

2. Materials and methods

The overall logical architecture and the sequential execution phases of the ABM are visually summarized in the flowchart presented.

2.1. Environment and Core Entities

The computational model is built upon a spatially explicit, discrete two-dimensional squared grid that represents the physical landscape where the simulation unfolds. The primary demographic units within this environment are autonomous agents A_i that stands for the people working in that environment. Agents A_i are organized into collective households defined as X_j. Within the simulation, the households H_j operates as the central socio-economic decision-making unit, managing both labor allocation and spatial positioning.

The physical presence of a household on the grid is anchored by a primary residential structure, defined as the house X_k. This structure occupies a single, specific coordinate cell (x_k, y_k) and serves as the spatial reference point for all distance calculations, social interactions, and agricultural expansions.

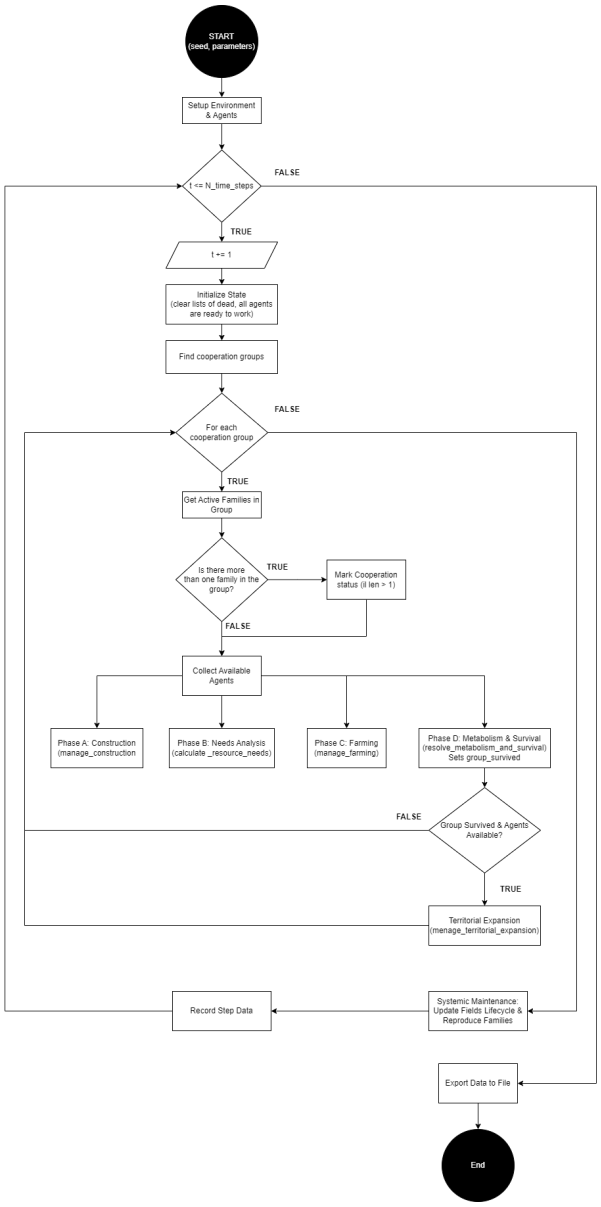

Figure 1: High-level flowchart of the ABM execution cycle, detailing the sequential phases of cooperation, agent allocation, metabolism, and spatial expansion.

To sustain themselves, households H must develop agricultural infrastructure, represented by fields F. Each F_l is a dynamic spatial entity characterized by a specific, localized fertility level, which dictates its potential caloric yield.

A family, its central house, and its continuously evolving network of associated fields collectively constitute a Farm X. Each farm X_p acts as the aggregate agricultural portfolio of the household. The spatial grid itself is managed dynamically by a terrain system that enforces strict topological constraints, ensuring that each discrete cell can be occupied by only one spatially-defined entity at a time.

2.2. Metabolic and Ecological Dynamics

The survival of each family unit is strictly dependent on its ability to satisfy the aggregate metabolic requirements of its members. At each discrete time step, every agent generates a caloric demand α, which the household H must meet by extracting resources from its agricultural assets. To fulfill this demand, available agents are deployed as agricultural labor β on the family's operational

fields. The extraction of calories is governed by a local ecological threshold, so that each field possesses a finite fertility level γ that determines its maximum potential energy yield *delta*. As labor is applied and calories are harvested, the field's fertility degrades proportionally to the extracted resources.

This continuous exploitation inevitably leads to soil exhaustion. When a field's fertility F_f is completely depleted, it transitions into a fallow state, rendering it temporarily unproductive. The fallow field must then undergo a strictly defined ecological recovery period

2.3. Spatial Settlement and Expansion Mechanisms

To sustain their growing population H_p, households H must continuously expand their agricultural footprint. This expansion is defined by a deterministic spatial algorithm that performs a concentric search, starting from the primary residential structure, to locate the nearest available grid cell for establishing a new field. This ensures both explainability and that agricultural infrastructure remains as contiguous and accessible as possible. However, as the population naturally increases, the household eventually reaches its maximum structural capacity. This demographic pressure triggers a mandatory scission event, forcing a subset of the family members to migrate and establish a new, independent settlement. The placement of this new household is not random across the global landscape, but is controlled by a proximity parameter η, which defines a specific maximum exploration radius around the parent settlement. The mechanism identifies all unoccupied spatial cells within this radius and allocates the new house accordingly.

2.4. The Urban Cohesion Index

To quantitatively assess the emergence of urban structures from the previously described expansion mechanics, we introduce the Urban Cohesion Index ω. Traditional density metrics often fail to capture the relational topology of settlements, treating uniformly dispersed populations similarly to clustered ones. Therefore, ω is specifically designed to evaluate spatial agglomeration by cross-referencing absolute physical distance with topological density, defined as distance rank. For a given set of n active household coordinates within the grid, the algorithm computes an $n \times n$ Euclidean distance matrix. Subsequently, a corresponding rank matrix is generated, which assigns an incremental ordinal rank to neighbors based on their proximity to each target household. The relational cohesion score between any two distinct households is formulated to be inversely proportional to the product of their normalized Euclidean distance and their normalized rank. ω is then derived by summing these individual matrix scores and applying a sample size normalization, yielding a final continuous value $\omega \in [0, 1]$. A score approaching 1 indicates maximum centralized density, where all units are perfectly clustered, whereas lower scores reflect high spatial fragmentation. By tracking the trajectory of this index over the simulation steps, the model could track phase transitions from dispersed rural patterns to cohesive urban agglomerations.

3. Experimental Setup and Scenario Analysis

To robustly evaluate the model and observe the macroscopic emergence of urban agglomerations, we conducted an extensive campaign of batch simulations. The experimental setup systematically explored the parameter space to identify phase transitions in the spatial behavior of the households. The analysis specifically focused on varying key parameters, as in Figure NNN.

A comprehensive overview of the primary parameters manipulated during the batch simulation phase is summarized in Table 1.

Data acquisition was designed to capture both collective phenomena and individual trajectories. At the macroscopic level, the simulation continuously recorded aggregate variables at each time step, including total population size, global food storage, the number of active agricultural fields, and the

Parameter Name	Description	Macro-Dynamic Influence
LABOR_PRODUCTIVITY	Caloric output generated by a single agent per work cycle.	Dictates baseline metabolic survival and global food storage capacity.
MAX_N_PERSONS_PER_FAMILY	Structural capacity limit of a single house before mandatory fission.	Acts as a demographic bottleneck, triggering spatial expansion when low.
FAMILY_SPLIT_RADIUS	Maximum distance allowed for placing a new house during a fission event.	Constrains spatial dispersion, forcing local density and cluster formation.
COOPERATION_MAX_DISTANCE	Maximum topological radius within which different families share labor and resources.	Accelerates the Urban Cohesion Index by incentivizing spatial convergence.
BIRTH_PROBABILITY	Baseline probability of a new agent being born in a household per time step.	Drives demographic pressure and accelerates household mortality when extreme.
AGENT_CALORIC_NEED	Fixed amount of calories consumed by each agent per time step.	Determines the aggregate metabolic pressure on the agricultural infrastructure.

Figure 2: Key experimental parameters manipulated during the batch simulation runs, detailing their specific functional definitions and systemic impacts on the model's macro-dynamics.

Urban Cohesion Index. Concurrently, microscopic data streams logged the precise life cycle, spatial coordinates, and resource accumulation of individual families, providing a high-resolution map of the demographic and spatial evolution. To ensure scientific reproducibility, each simulation run was initialized with a specifically recorded random seed, allowing for the exact reconstruction of stochastic events and the isolated observation of specific parametric effects. This massive generation of simulated longitudinal data provided the necessary statistical foundation to correlate localized micro-behaviors with macro-spatial urban outcomes.

.

4. Results

4.1. Population and Resource Dynamics

In scenarios characterized by low labor productivity or highly constrained initial fertility, the system frequently experiences a premature demographic collapse. In these instances, isolated households are unable to overcome the vital caloric debt, leading to early starvation events that prevent any meaningful settlement expansion.

However, even when initial conditions allow for successful colonization and massive demographic growth, the environment remains highly vulnerable to ecological thresholds. If the rapid population expansion outpaces the recovery capacity of the agricultural infrastructure, the system falls into a severe 'overshoot and collapse' trajectory. A spatial visualization of this specific dynamic—where the population completely saturates the grid before ultimately suffering a systemic starvation event and total extinction—is illustrated in 3.

Conversely, when baseline agricultural parameters allow sustainable resource extraction, the global population exhibits rapid initial growth followed by a stabilization phase. During this stabilization, the aggregate food storage acts as a buffer against localized soil exhaustion. This demographic sustainability is the prerequisite for spatial complexity, as only environments that support a critical mass of active households generate the spatial pressure necessary for structural reorganization.

The structural relationship between demographic growth and resource accumulation is further shown by mapping total population against global food storage. While a strict, positive linear correlation dominates the macro-scale—indicating a standardized metabolic requirement—the system exhibits significant instability at lower demographic levels. For populations under $1,500$ units, the data reveals a high-variance cluster with food reserves falling well below the main trendline. This variance reflects the

Figure 3: Visual progression of an "overshoot and collapse" scenario within the spatial grid. From left to right: (1) Initial colonization with abundant fertile land; (2) Intermediate expansion and structural clustering; (3) Peak demographic saturation and extreme metabolic stress; (4) Systemic starvation event resulting in total population collapse and a landscape of exhausted fallow fields.

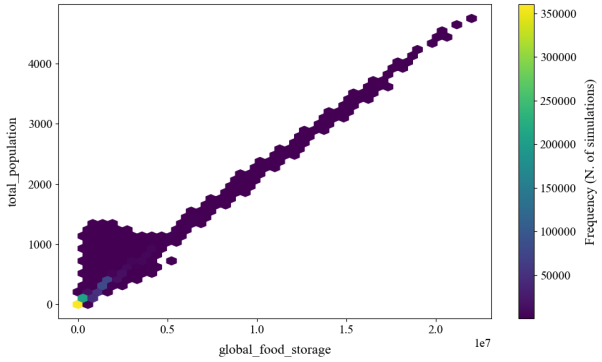

Figure 4: Total population versus global food storage. A threshold at 1,500 units marks a phase transition, from a first vulnerable, high-variance resource accumulation phase to a second highly resilient, standardized linear scaling phase.

metabolic vulnerability and relative inefficiency of small, isolated rural households. However, once the population surpasses this critical threshold of 1,500, the variance collapses and the data aligns perfectly along the primary accumulation axis. This phenomenon highlights a clear systemic resilience achieved through critical demographic mass, where aggregate food storage scales up robustly to the order of tens of millions, buffering the urbanizing population against localized ecological exhaustion.

4.2. Phase Transition in Urban Cohesion

The most significant findings emerge from the temporal analysis of the Urban Cohesion Index ω. The data demonstrate that urbanization within the model does not occur as a gradual, linear progression, but exhibits clear phase transitions. In the early stages of simulation, the index remains remarkably low, reflecting a highly fragmented landscape of isolated farms driven by the demographic fission mechanism. However, as the spatial grid reaches a critical saturation point—where the distance between newly founded settlements and existing infrastructure minimizes—ω undergoes a sudden and exponential increase. This spike quantitatively marks the structural collapse of the dispersed rural pattern and the spontaneous self-organization of dense, centralized urban cores.

Furthermore, the scatter plot analysis relating total population to ω reveals a distinct non-linear regime shift. The data identifies a critical spatial threshold around a cohesion value of 0.6; below this point, populations remain universally constrained to low numbers (under 500 individuals). However, crossing this 0.6 threshold unlocks massive demographic variability, allowing the system to sustain populations up to 5000 units, peaking between cohesion $0.7 < \omega < 0.8$. Interestingly, extreme cohesion ($\omega > 0.8$) does not correlate with further population growth, suggesting an upper metabolic limit to extreme urban density.

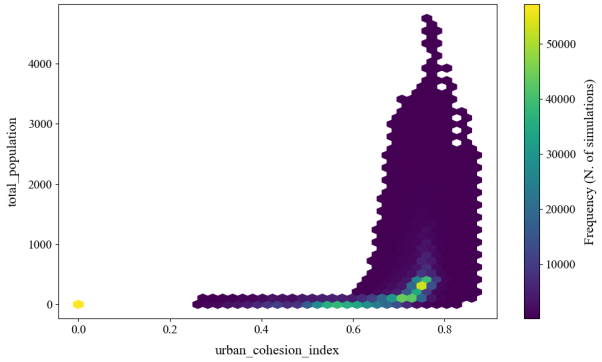

Figure 5: Scatter plot of P against ω. A critical spatial threshold at 0.6 triggers a non-linear regime shift, unlocking massive demographic growth that peaks between 0.7 and 0.8 before reaching an upper metabolic limit at extreme densities.

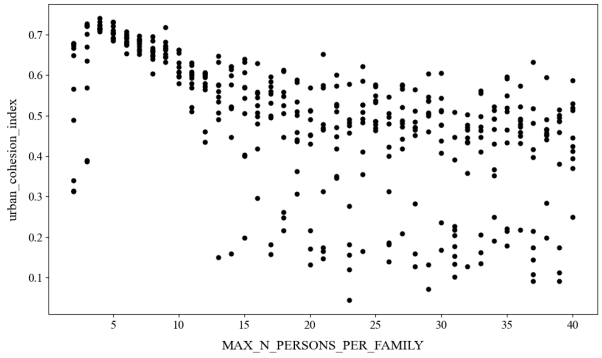

Figure 6: Urban Cohesion Index ω versus maximum household capacity. The data reveals optimal spatial clustering for small households (3-4 individuals) and extreme spatial fragmentation for limits exceeding 15 individuals.

The underlying mechanics of this demographic bottleneck are fully shown when correlating the maximum household capacity directly with ω. The distribution of these data points clearly presents two distinct regimes. In the high-cohesion regime—characterized by strict capacity limits between 2 and 15 individuals—the system exhibits remarkable spatial order. Cohesion peaks optimally ($\omega > 0.7$) for small family units of 3 to 4 individuals. This strict limitation on household size continuously forces proximity-constrained fission events, which organically generate the dense spatial clustering necessary for macro-level urban aggregation. Conversely, allowing a capacity greater than 15 individuals shifts the system into a regime of high structural entropy. In this state, the cohesion index fragments into a highly dispersed, unpredictable cloud, frequently collapsing to minimal values ($0.1 < \omega < 0.3$). This spatial disintegration confirms that oversized households suppress the cooperative clustering required to optimize resource extraction, leading to a fragmented and fragile landscape.

4.3. Triggers of Agglomeration

The batch scenario analysis further isolates the specific parameters that accelerate or delay this phase transition. The maximum cooperation distance plays a pivotal role; scenarios with a broader cooperation radius consistently exhibit earlier and more pronounced spikes in ω, as households H actively cluster to deal with collective labor and share caloric surpluses. Furthermore, the households split radius acts as a strong spatial constraint. When the split radius is tightly restricted, newly formed H are forced to settle in immediate proximity to their parent structures, accelerating local density. The relationship between these parameters confirms that early urbanization, as captured by the cohesion index, is an

emergent response at a system level driven by the need to balance metabolic survival with extreme spatial competition.

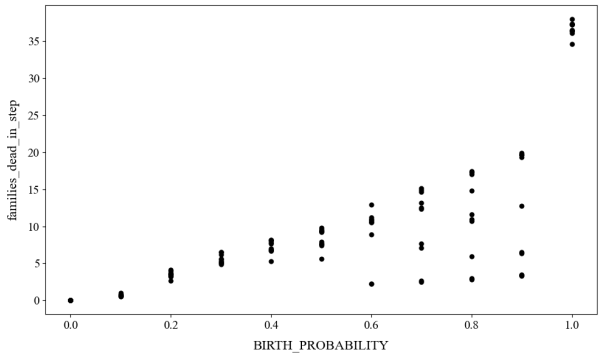

Figure 7: Impact of birth probability on household mortality. Unconstrained natality triggers a non-linear spike in family failures, highlighting the strict ecological limits and the self-regulating nature of the simulated ecosystem.

The analysis of specific demographic parameters further highlights the ecological limits of the simulated environment. By plotting the baseline birth probability against the number of household failures per time step, a clear non-linear relationship emerges. At lower birth probabilities, family mortality remains predictably stable. However, as the birth probability increases, the system exhibits severe heteroskedasticity, with the variance in household failure rates expanding drastically. This trend culminates in a qualitative breaking point at the maximum probability threshold (which is 1.0), where household mortality spikes abruptly to nearly double the rate observed at 0.9. Taken together with the previous macro-dynamics, these results portray a highly complex, self-regulating ecosystem: while spatial cohesion unlocks population growth and demographic mass stabilizes resource storage, unconstrained natality inevitably triggers accelerated household mortality due to extreme spatial and metabolic saturation.

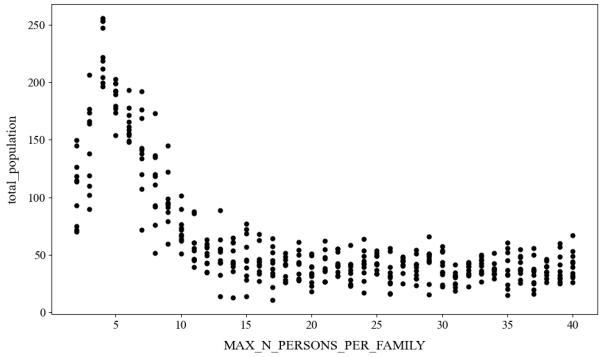

Figure 8: Relationship between maximum family size and global population. The data reveals a counterintuitive dynamic where small, highly constrained households (4-5 members) maximize total carrying capacity, while larger family structures prove inherently inefficient for systemic demographic growth.

Further parametric analysis reveals a highly counterintuitive dynamic regarding household population capacity. By correlating the maximum allowed persons per family with the total sustained population, a severe bottleneck effect becomes evident. The data demonstrates a peak systemic efficiency when the household limit is highly constrained, specifically between 4 and 5 individuals, allowing the global population to maximize its carrying capacity. However, as the maximum family size exceeds this narrow optimum, the system experiences drastic diminishing returns; at a limit of 10 persons, the maximum achievable population H_p is effectively halved, and for limits between 15 and 40, the global population stabilizes at a severely depressed plateau. This phenomenon indicates that oversized households are

inherently inefficient within the model's ecological constraints. Large families concentrate caloric demand in localized areas, rapidly exhausting nearby soil fertility and increasing the risk of massive starvation events. Conversely, artificially restricting household size acts as a catalyst for continuous demographic fission, forcing an aggressive spatial expansion that optimizes global resource extraction and ensures greater systemic resilience.

5. Discussion and Conclusions

The computational experiments presented in this study provide a quantitative demonstration of how macro-level urban agglomerations can spontaneously emerge from micro-founded, decentralized household decisions. By utilizing the Urban Cohesion Index ω, we were able to observe that the transition from a dispersed agricultural landscape to a centralized urban structure is not a gradual, linear consequence of population growth. Rather, it manifests as a sudden phase transition triggered by spatial saturation and metabolic constraints. When the availability of highly fertile, unoccupied land dwindles due to continuous demographic fission and localized ecological degradation, spatial clustering ceases to be merely an option and becomes a systemic necessity for survival. Also, the demographic sustainability appears to be a prerequisite for spatial complexity. Finally, the model illustrates that early urbanization is fundamentally an adaptive response to environmental pressure, where proximity and cooperation optimize resource extraction and mitigate the risks of starvation.

These findings carry theoretical implications for the understanding of early spatial economies and urban settings, reinforcing the perspective that the first permanent settlements were complex, self-organizing adaptive systems. The dynamics observed in our simulations suggest that physical agglomeration is deeply intertwined with the life cycle of the surrounding agricultural infrastructure. The necessity to balance the ecological recovery of fallow fields with immediate caloric demands forces populations to negotiate their spatial distribution, ultimately driving them toward dense, cooperative hubs when spatial expansion is no longer viable.

Despite these insights, the current model possesses many limitations that offer clear avenues for future research. Primarily, the simulated landscape is topologically isotropic, lacking geographical features such as water sources, natural barriers, or variations in baseline soil quality, which historically dictated the placement of early cities. Additionally, the agents in our model exhibit homogeneous behavioral rules. Real-world social systems are characterized by heterogeneous preferences, varied risk aversions, and the eventual emergence of specialized, non-agricultural labor. Also, there is a single source of calories, and no meteorological or seasonal event are included. Finally, households are never in conflict, and the urban settlements is a purely emergent result of the metabolic need, while in literature it is suggested it could have depended also from the need for a common and more organized defense [1].

Future extensions of this framework should introduce environmental heterogeneity and socio-economic stratification to observe how unequal resource distribution affects ω. Furthermore, incorporating technological shocks, such as innovations in farming tools that alter labor productivity mid-simulation, could provide deeper insights into the resilience and evolution of these early urban centers.

References

[1] P. Turchin, et al., Ultrasociety how 10,000 years of war made humans the greatest cooperators of earth (2016).

[2] M. Burtsev, P. Turchin, Evolution of cooperative strategies from first principles, Nature 440 (2006) 1041–1044.

[3] G. Hardin, Extensions of" the tragedy of the commons", Science 280 (1998) 682–683.
[4] E. Lecoutere, L. Jassogne, Fairness and efficiency in smallholder farming: The relation with intrahousehold decision-making, The Journal of Development Studies 55 (2019) 57–82.
[5] G. B. West, J. H. Brown, Life's universal scaling laws, Physics today 57 (2004) 36–42.
[6] L. M. Bettencourt, J. Lobo, D. Helbing, C. Kühnert, G. B. West, Growth, innovation, scaling, and the pace of life in cities, Proceedings of the national academy of sciences 104 (2007) 7301–7306.
[7] C. Berceanu, F. Bertolotti, N. Arshad, M. Patrascu, Understanding the mechanisms of infodemics: Equation-based vs. agent-based models, Plos one 20 (2025) e0338614.
[8] F. Bertolotti, R. Occa, "roads? where we're going we don't need roads." using agent-based modeling to analyze the economic impact of hyperloop introduction on a supply chain, in: European Conference on Multi-Agent Systems, Springer, 2020, pp. 493–500.
[9] F. Bertolotti, S. Roman, The evolution of risk sensitivity in a sustainability game: an agent-based model., in: WOA, 2022, pp. 101–115.
[10] F. Bertolotti, S. Roman, Risk sensitive scheduling strategies of production studios on the us movie market: An agent-based simulation, Intelligenza Artificiale 16 (2022) 81–92.
[11] R. Occa, F. Bertolotti, et al., Understanding the effect of iot adoption on the behavior of firms: An agent-based model, in: CS & IT Conference Proceedings, volume 12, CS & IT Conference Proceedings, 2022.
[12] R. M. Dawes, Social dilemmas., Annual review of psychology (1980).
[13] M. Marsili, D. Challet, R. Zecchina, Exact solution of a modified el farol's bar problem: Efficiency and the role of market impact, Physica A: Statistical Mechanics and its Applications 280 (2000) 522–553.
[14] F. Bertolotti, N. Kadera, L. Pasquino, L. Mari, An epidemiological extension of the el farol bar problem, Frontiers in Big Data 8 (2025) 1519369.
[15] H. Rahmandad, J. Sterman, Heterogeneity and network structure in the dynamics of diffusion: Comparing agent-based and differential equation models, Management science 54 (2008) 998–1014.
[16] R. L. Axtell, J. M. Epstein, J. S. Dean, G. J. Gumerman, A. C. Swedlund, J. Harburger, S. Chakravarty, R. Hammond, J. Parker, M. Parker, Population growth and collapse in a multiagent model of the kayenta anasazi in long house valley, Proceedings of the National Academy of Sciences 99 (2002) 7275–7279.
[17] A. Piras, F. Bertolotti, How risk preferences shape city-state success: An agent-based model of resource management., in: WOA, 2024, pp. 283–297.
[18] T. Filatova, P. H. Verburg, D. C. Parker, C. A. Stannard, Spatial agent-based models for socio-ecological systems: Challenges and prospects, Environmental modelling & software 45 (2013) 1–7.
[19] J. M. Epstein, Generative social science: Studies in agent-based computational modeling, Princeton University Press, 2012.
[20] Y. Song, Y. Long, P. Wu, X. Wang, Are all cities with similar urban form or not? redefining cities with ubiquitous points of interest and evaluating them with indicators at city and block levels in china, International Journal of Geographical Information Science 32 (2018) 2447–2476.
[21] G. Dumedah, E. K. Garsonu, Characterising the structural pattern of urban road networks in ghana using geometric and topological measures, Geo: Geography and Environment 8 (2021) e00095.